Excitons in silicon diodes and solar cells: A threeparticle theory

Richard Corkish, Daniel S.P. Chan, and Martin A. Green

Articles you may be interested in
Tunable vibrational band gaps in one-dimensional diatomic granular crystals with three-particle unit cells
J. Appl. Phys. **109**, 074906 (2011); 10.1063/1.3556455

A reformulation of simple liquids theory—Renormalization by one-, two-, and three-particle densities
J. Math. Phys. **39**, 2077 (1998); 10.1063/1.532277

An integrable threeparticle system
J. Math. Phys. **35**, 1219 (1994); 10.1063/1.530585

The threeparticle S matrix
J. Math. Phys. **15**, 338 (1974); 10.1063/1.1666649

Born—Oppenheimer Separation for ThreeParticle Systems. I. Theory
J. Chem. Phys. **45**, 3806 (1966); 10.1063/1.1727403

Excitons in silicon diodes and solar cells: A three-particle theory

Richard Corkish,[a)] Daniel S.-P. Chan,[b)] and Martin A. Green

Centre for Photovoltaic Devices and Systems, University of New South Wales, Sydney, Australia 2052

Recent work has indicated that a significant number of electrons and holes remain in the free-exciton form in silicon at room temperature, a finding which, if supportable by experimental evidence, requires the inclusion of excitons in diode and solar cell theory. Excitons, although neutral, may contribute to device currents by diffusing to the junction region where they may be dissociated by the field. A generalized three-particle theory of transport in semiconductors is presented. The results of application of the theory to silicon devices indicate a decrease in the dark saturation current as well as an increase in light-generated current when excitons are incorporated in the theory so long as exciton diffusion length exceeds that of the minority carriers. The work includes suggestions for experimental methods to confirm exciton involvement and to estimate the value of the exciton-binding parameter from spectral response measurements on solar cells. © *1996 American Institute of Physics.* [S0021-8979(96)00701-9]

I. INTRODUCTION

Although exciton diffusion has been proposed as an important transport mechanism in organic photovoltaic cells,[1] excitons have, to date, been neglected in room-temperature diode and inorganic solar cell theory for two reasons. Most importantly, it has been considered that exciton populations in semiconductors at room temperature and above are insignificant.[2] This view has been challenged by Hangleiter and Pilkuhn[3] and by Kane and Swanson,[4] who suggest that free-exciton densities in silicon at room temperatures can approach those of minority carriers. In Fig. 1 we show the ratio of exciton and minority carrier populations in silicon in low injection at 300 K, according to Kane and Swanson.[4] Increasing majority carrier concentration enhances screening of the Coulomb interaction between the electrons and holes which constitute the excitons and their binding energy is consequently reduced. This affects the population statistics, as indicated in Fig. 1. The decrease of the excitons' binding energy to zero corresponds to Mott's[5] insulator–metal transition and bound excitons cannot exist at higher majority carrier densities. For silicon in low injection the Mott density is[4] 1.03×10^{18} cm^{-1}. The second reason for the neglect of excitons is that they are neutral and cannot, *per se*, contribute to current.[6] However, should an exciton diffuse to the *pn* junction region in a diode or solar cell it is likely to be dissociated by the strong electric field into its constituent carriers and is then able to contribute.[4]

Together, the possibility of significant exciton populations at room temperature, their probable involvement in current generation, and their proposed role in recombination[7] suggest the need for the inclusion of excitons in diode and solar cell theory.[8,9] In this article, we formulate a three-particle theory, including exciton transport, and incorporate it into the theory for (i) a dark diode, and (ii) a solar cell whose base is assumed to be of infinite thickness and in which optical generation is assumed independent of position. In

Sec. III we apply the theory to silicon devices at 300 K and propose an experimental technique to both confirm the contribution of exciton transport to current and to estimate the value of an important exciton binding parameter.

Our numerical results suggest a significant decrease in dark saturation current and simultaneous increase in short circuit current may be possible if exciton contributions are optimized and if exciton diffusion length exceeds that for minority carriers. However, confidence in the numerical results is limited by the lack of experimental values for exciton parameters at room temperature.

II. THEORY

A. Three-particle formulation

The three-particle (electron, hole, and exciton) theory outlined here was proposed by Green[8] and further developed by Chan.[9] The inclusion of excitons requires an additional term in each of the current continuity equations to account for the binding of carrier pairs into excitons:

$$(1/q)\nabla \cdot J_n = U_{eh} - G_{eh} + B \tag{1}$$

$$(1/q)\nabla \cdot J_p = -U_{eh} + G_{eh} - B, \tag{2}$$

where U_{eh} is the net recombination rate for electrons and holes (not preceded by exciton formation), G_{eh} is the rate of direct generation of carrier pairs (nonexcitonic) by external disturbances such as light, and B is the net rate at which electrons and holes bind together to form excitons. Additionally, we require a similar equation for the continuity of exciton flow, Φ

$$\nabla \cdot \Phi = -U_x + G_x + B, \tag{3}$$

where U_x is the exciton recombination rate and G_x is the rate of exciton generation by external disturbances such as light. Since excitons, being neutral, may flow only by diffusion, we have the following expression for excitonic flux:

$$\Phi = -D_x \nabla \cdot n_x, \tag{4}$$

where D_x is the diffusion coefficient for excitons.

[a)]Electronic mail: r.corkish@unsw.edu.au
[b)]Current address: Department of Mathematics, Massachusetts Institute of Technology, Cambridge, MA 02139.
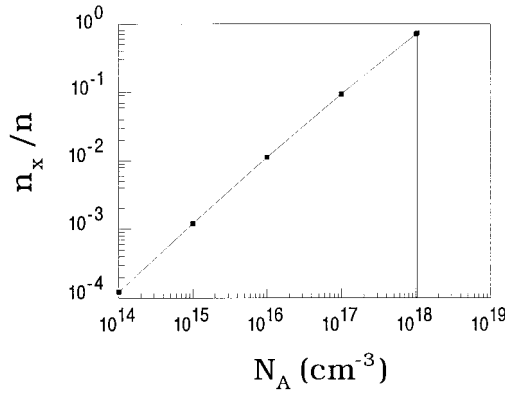
FIG. 1. Ratio of exciton and minority carrier concentrations in silicon in low injection at 300 K. Data is from Kane and Swanson,[4] Eq. (27). The ratio increases with doping density up to the Mott density at 1.03×10^{18} cm^{-3}.

The recombination terms can be most simply expressed in terms of lifetimes $U_{eh} = \Delta n/\tau_n = \Delta p/\tau_p$ and $U_x = \Delta n_x/\tau_x$, where $\Delta n, \Delta p, \Delta n_x$ are the excess electron, hole, and exciton concentrations, τ_n, τ_p, τ_x are the electron, hole, and exciton lifetimes with respect to recombination. The generation rates vary exponentially with distance from the surface: $G_{eh} = G_{eh0} \exp(-\alpha z)$ and $G_x = G_{x0} \exp(-\alpha z)$, where G_{eh0} and G_{x0} are the carrier and exciton generation rates at the semiconductor surface, α is the absorption coefficient with all absorption processes (creation of electron-hole pairs and excitons and free-carrier absorption) considered and z is the distance into the semiconductor. From the law of mass action, the binding rate is given by[9,10]

$$B = b(np - n^* n_x),\tag{5}$$

where b is a coefficient for binding of carriers into excitons, n^* is an equilibrium constant,[11] and n_x is the density of excitons. This formulation implicitly assumes that carrier $\leftrightarrow$ exciton reactions occur more rapidly than recombination and generation processes. An equilibrium between carriers and excitons may not be possible in direct gap semiconductors with short radiative lifetimes.[4]

B. Simplified diode and solar cell model

We use a one-sided, abrupt-junction, wide-base diode model and generally follow the standard development of the theory for dark and illuminated diodes in the form outlined by Green.[12] We adopt the five main approximations stated and justified therein

(1) The depletion approximation.
(2) Within the depletion region the drift and diffusion currents are opposing and approximately equal in magnitude.
(3) Low-level injection is assumed.
(4) Minority carriers in bulk regions are assumed to flow predominantly by diffusion.
(5) Recombination in the depletion region is neglected.

Additionally, in our model we neglect the thin emitter layer of the cell ("one-sided" junction model) and consider only the base region, which we assume to be p-type. An

electron will be collected (will contribute to current) if it diffuses to the edge of the depletion region at $z=0$. Similarly, if an exciton diffuses to the same plane or to a contact, it is assumed to be dissociated into an electron and a hole and to contribute to current. The analysis is one dimensional and all surface effects are neglected. The generalized theory is, of course, able to address less restricted situations.

C. Simplified theory including excitons

Since diffusion is assumed to be the predominant transport mechanism for minority carriers in the bulk and the only transport mechanism for excitons, we combine the modified continuity equations [Eqs. (1)–(3)] with Eq. (4) and the electron current density equation to produce the following coupled pair of differential equations (in one dimension) for p-type bulk semiconductor:

$$D_n \frac{d^2 \Delta n}{dz^2} = \frac{\Delta n}{\tau_n} + b(\Delta n N_A - \Delta n_x n^*) - G_{eh} \exp(-\alpha z)\tag{6}$$

and

$$D_x \frac{d^2 \Delta n_x}{dz^2} = \frac{\Delta n_x}{\tau_x} - b(\Delta n N_A - \Delta n_x n^*) - G_x \exp(-\alpha z),\tag{7}$$

where D_n and D_x are the diffusion coefficients for electrons and excitons, respectively. We are able to change from the total concentration to the excess concentration variables since $np = n_x n^*$ by the law of mass action when the electron–exciton system is in equilibrium. The $z=0$ plane is defined at the p-type edge of the depletion region and, hence, the boundary conditions[12] are $n(z=0) = n_{p0} \exp(qV_a/kT)$ and $n_x(z=0) = n_{x0}$, where $n_{p0} \approx n_i^2/N_A$, n_i is the intrinsic carrier concentration, V_a is the applied forward voltage, n_{x0} is the equilibrium exciton concentration and $kT/q = 25.85$ mV at 300 K. At the other boundary, $z=\infty$, the electron and exciton densities must be finite.

We express Eqs. (6) and (7) in matrix form,

$$\frac{d^2}{dx^2} \begin{bmatrix} \Delta n \\ \Delta n_x \end{bmatrix} = \begin{bmatrix} M_{11} & M_{12} \\ M_{21} & M_{22} \end{bmatrix} \begin{bmatrix} \Delta n \\ \Delta n_x \end{bmatrix} + \begin{bmatrix} \Gamma_n(z) \\ \Gamma_x(z) \end{bmatrix},\tag{8}$$

where

$$M_{11} = (1/\tau_n + bN_A)/D_n,$$
$$M_{12} = -bn^*/D_n,$$
$$M_{21} = -bN_A/D_x,$$
$$M_{22} = (1/\tau_x + bn^*)/D_x,\tag{9}$$
$$\Gamma_n(z) = -G_{eh} \exp(-\alpha z)/D_n,$$
$$\Gamma_x(z) = -G_x \exp(-\alpha z)/D_x,$$

and use standard eigenvalue–eigenvector techniques[13] to solve the coupled differential equations. The characteristic polynomial of M, the matrix containing M_{ij}, is

$$\chi(\epsilon) = \det(M - \epsilon I) = \epsilon^2 - (M_{11} + M_{22})\epsilon + M_{11}M_{22} - M_{21}M_{12},\tag{10}$$

where I is the identity matrix and its discriminant is $\delta = M_\Delta^2 + 4M_{12}M_{21}$, where $M_\Delta = M_{11} - M_{22}$. The two eigenvalues, $\epsilon_\pm$, are the roots of the characteristic polynomial

$$\epsilon_\pm = 0.5[M_{11} + M_{22} \pm \delta^{1/2}]. \tag{11}$$

In order to find physical meanings for these terms, we consider the decoupled ($b=0$) case, in which $\epsilon_\pm = M_{11}, M_{22}$, and $M_{11} = L_n^{-2}$ and $M_{22} = L_x^{-2}$, where $L_n = (D_n \tau_n)^{1/2}$ and $L_x = (D_x \tau_x)^{1/2}$. In "exciton-dominant" systems, where $M_{11} > M_{22}, M_{11}$ must equal the larger eigenvalue, ϵ_+, but in electron-dominant systems, where $M_{11} < M_{22}, M_{11} = \epsilon_-$. Consequently, in an exciton-dominant system we call $\epsilon_+^{1/2}$ the effective inverse diffusion length for electrons accounting for excitons ($1/L_n'$) and $\epsilon_-^{1/2}$ the effective inverse diffusion length for excitons accounting for electrons ($1/L_x'$). In electron-dominant systems these designations are swapped.

1. Homogeneous (dark) solution

The homogeneous solutions, which correspond to a diode in the dark ($\Gamma_n = \Gamma_x = 0$), may be used to find the saturation current density, J_0. The homogeneous solutions are (see Appendix)

$$\Delta n = 0.5\delta^{-1/2}[(\delta^{1/2} + M_\Delta)\exp(-\epsilon_+^{1/2}z) + (\delta^{1/2} - M_\Delta)$$
$$\times \exp(-\epsilon_-^{1/2}z)]n_{p0}\exp(qV_a/kT) \tag{12}$$

and

$$\Delta n_x = M_{21}\delta^{-1/2}[\exp(-\epsilon_+^{1/2}z)$$
$$- \exp(-\epsilon_-^{1/2}z)]n_{p0}\exp(qV_a/kT). \tag{13}$$

The current density in a dark cell consists, since we neglect majority carrier current in the one-sided model, of flows of electrons and dissociating excitons. This is found by adding the flows at the $z=0$ plane

$$J_n = qD_n dn/dz|_{z=0} + qD_x dn_x/dz|_{z=0}$$
$$= -0.5qD_n\{\epsilon_+^{1/2}[1 + (M_\Delta + 2rM_{21})\delta^{-1/2}]$$
$$+ \epsilon_-^{1/2}[1 - (M_\Delta + 2rM_{21})\delta^{-1/2}]\}n_{p0}\exp(qV_a/kT), \tag{14}$$

where $r = D_x/D_n$. Hence, the dark saturation current is

$$J_0 = -0.5qD_n\{\epsilon_+^{1/2}[1 + (M_\Delta + 2rM_{21})\delta^{-1/2}]$$
$$+ \epsilon_-^{1/2}[1 - (M_\Delta + 2rM_{21})\delta^{-1/2}]\}n_{p0}. \tag{15}$$

This is to be compared to the corresponding expression when excitons are neglected (see Green,[12] p. 75):

$$J_0' = -qn_{p0}D_n/L_n, \tag{16}$$

where L_n is the electron diffusion length. Numerical values from these equations are compared in Sec. III B 1.

2. Inhomogeneous (illuminated) solution

The inhomogeneous solution, for which either or both electron and exciton optical generation are non-zero, yields the light-generated current if the short circuit condition is applied. To solve Eq. (8) when Γ_n and/or Γ_x are finite, we first find a particular solution which is given by (see Appendix)

$$\Delta n_{\text{partic}} = \exp(-\alpha z)/\chi(\alpha^2)[(M_{22} - \alpha^2)G_{eh}/D_n$$
$$- M_{12}G_x/D_x] \tag{17}$$

and

$$\Delta n_{x,\text{partic}} = \exp(-\alpha z)/\chi(\alpha^2)[(M_{11} - \alpha^2)G_x/D_x$$
$$- M_{21}G_{eh}/D_n], \tag{18}$$

where $\chi(\alpha^2)$ is found from Eq. (10). In each of Eqs. (17) and (18) the first term in brackets is concerned with optical generation of the relevant particles and the second is describing the effects of the interaction between exciton and electron populations.

The particular solution is added to the homogeneous solution and the boundary conditions for short circuit are applied to yield

$$\Delta n = R \cdot \exp(-\epsilon_+^{1/2}z) + S \cdot \exp(-\epsilon_-^{1/2}z) + \Delta n_{\text{partic}} \tag{19}$$

and

$$\Delta n_x = \gamma R \cdot \exp(-\epsilon_+^{1/2}z) + \eta S \cdot \exp(-\epsilon_-^{1/2}z) + \Delta n_{x,\text{partic}}, \tag{20}$$

where

$$R = \{G_{eh}/D_n[\eta(M_{22} - \alpha^2) + M_{21}]$$
$$- G_x/D_x(\eta M_{12} + M_{11} - \alpha^2)\}M_{12}/[\delta^{1/2}\chi(\alpha^2)] \tag{21}$$

$$S = -\{G_{eh}/D_n[\gamma(M_{22} - \alpha^2) + M_{21}]$$
$$- G_x/D_x(\gamma M_{12} + M_{11} - \alpha^2)\} \tag{22}$$

$$\gamma = 0.5[(M_\Delta^2 + 4M_{12}M_{21})^{1/2} - M_\Delta]/M_{12} \tag{23}$$

$$\eta = -0.5[(M_\Delta^2 + 4M_{12}M_{21})^{1/2} + M_\Delta]/M_{12}. \tag{24}$$

Differentiation of Eqs. (19) and (20) then gives the light-generated current density

$$J_L = qD_n dn/dz|_{z=0} + qD_x dn_x/dz|_{z=0}$$
$$= -qD_n(R\epsilon_+^{1/2} + S\epsilon_-^{1/2} + \Delta n_{\text{partic}}\alpha)$$
$$- qD_x(\gamma R\epsilon_+^{1/2} + \eta S\epsilon_-^{1/2} + \Delta n_{x,\text{partic}}\alpha). \tag{25}$$

For comparison, the light-generated current density when excitons are neglected is given by

$$J_L' = qG_{eh}/(\alpha + L_n^{-1}). \tag{26}$$

III. APPLICATION TO SILICON DEVICES

A. Parameter values

A total generation rate at the surface, $G_{\text{total0}} = G_{eh0} + G_{x0}, = 10^{10}$ cm^{-3} was assumed for all illuminated cases. The illuminated solar cell was modeled with $\alpha = 0$ in order to simulate constant generation rate throughout, corresponding to the case of illumination by weakly absorbed light.

1. Electron parameters

Kane and Swanson[4] suggest that the exciton theory can account for an effective increase in n_i at doping densities below the Mott transition, similar to the result of band gap narrowing above that transition. We have excluded this apparent band gap narrowing from our formulation since it has

J. Appl. Phys., Vol. 79, No. 1, 1 January 1996

Corkish, Chan, and Green 197

no effect on the current ratios we present. However, this effect is included in our spectral response calculations, discussed in Sec. III A 4. We assume a value[14] of 1.00×10^{10} cm^{-3} for the intrinsic carrier concentration at 300 K. Electron lifetime is assumed to vary with doping according to the following empirical relationship[15]

$$\tau_n(N_A) = \tau_n(0)/(1 + N_A/7.10 \times 10^{15}) \text{s}, \qquad (27)$$

where $\tau_n(0) = 1.70 \times 10^{-5}$. Electron diffusion coefficient variation with doping was obtained from an empirical fit to a model for minority electron mobility as a function of doping density.[16]

2. Exciton parameters

For the unscreened exciton binding energy (appropriate for intrinsic material) we use the result of wavelength-derivative absorption measurements[17] at 1.8 K multiplied by 1.4 to account for the different effective masses at our temperature of 300 K. This yields an unscreened exciton binding energy of $E_{x\infty} = 20.6$ meV.[18] Increasing majority carrier densities screen the exciton energy until eventually, at the Mott[19] density, the binding energy goes to zero and excitons cease to exist. For the case of low injection, this majority carrier density is[4] $n_{\text{Mott}} = 1.03 \times 10^{18}$ cm^{-3} if we assume that the expression derived by Norris and Bajaj,[20] which was verified only for $T < 80$ K, may be used at 300 K. Hence, the binding energy as a function of doping is then given by[4]

$$E_x(N_A) = E_{x\infty}[1 - (N_A/n_{\text{Mott}})^{1/2}]^2. \qquad (28)$$

This may be used to find

$$n^*(N_A) = \exp[-E_x(N_A)/kT](N_C N_V)^{1/2}/f, \qquad (29)$$

where we adopt Kane and Swanson's values of $f \sim 21$ and $(N_C N_V)^{1/2} \approx 3 \times 10^{19}$. The exciton lifetime for intrinsic material, $\tau_x(0)$, at 300 K was calculated[10] by the principle of detailed balance to be equal to 100 μs, which may be regarded as an upper bound. In this work, we assume that τ_x varies with doping in proportion to τ_n and investigate (see Sec. B 3, below) the effect of varying $\tau_x(0)$. Hence, τ_x is given by Eq. (27) when $\tau_x(0)$ replaces $\tau_n(0)$. However, that expression does not account for the excitonic Auger mechanism in which free excitons are destroyed at deep impurity sites[7] and exciton lifetimes may actually be shorter than assumed here. For the exciton diffusion coefficient we follow Kane and Swanson[4] in extrapolating to 300 K the empirical expression obtained[21] for $T < 20$ K, resulting in $D_x = 17$ cm^2 s^{-1}. In the absence of experimental data, the diffusion coefficient is assumed independent of doping density since excitons are neutral particles.

On the basis of a model[22] for the thermal capture of electrons into traps, Nolle[10] assumes the following variation of the exciton binding parameter, b, with temperature

$$b = 10^{-3}T^{-2} + 2.5 \times 10^{-6}T^{-1/2} + 1.5$$
$$\times 10^{-7} \quad (\text{cm}^3 \text{ s}^{-1}). \qquad (30)$$

This gives a value of 3×10^{-7} at 300 K, in approximate agreement with the value of 7×10^{-7} obtained by extrapolating the theoretical expression, $b = 1.14 \times 10^{-5}T^{-1/2}$, obtained by Barrau et al.[23] for $4 < T < 15$ K. In this article, we treat b
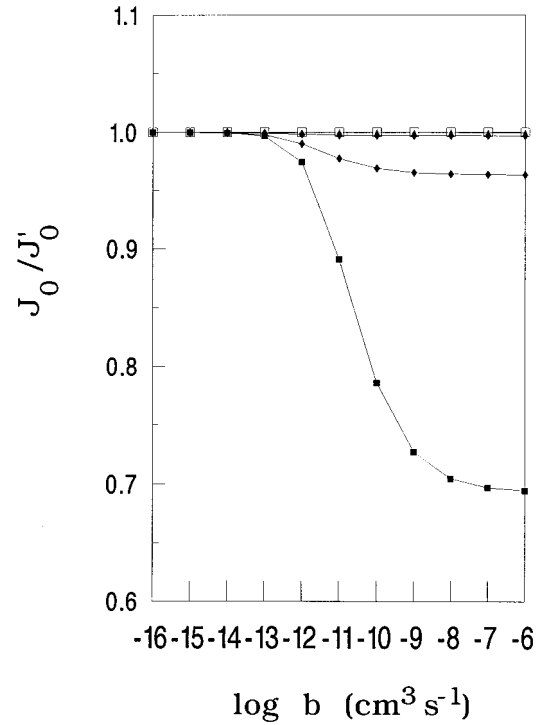

FIG. 2. Ratio of dark saturation current density with excitons considered to that with excitons neglected as a function of the binding coefficient. The parameter is the doping density, N_A (cm^{-3}): unfilled squares, 10^{15}; triangles, 10^{16}; diamonds, 10^{17}; filled squares, 10^{18}.

as a variable for two reasons. Firstly, it allows us to confirm that when $b \to 0$ our calculated currents relax towards the values expected from theory which neglects excitons and, secondly, we lack any experimental evidence for the value of b.

B. Effect of excitons on device currents

1. Dark saturation current

The dark saturation current was calculated by Eq. (15) with excitons considered and by Eq. (16) with excitons neglected, assuming $\tau_x(0) = 10^{-4}$ s. The ratio of these currents is shown in Fig. 2 as a function of the binding coefficient, b, and with the doping density as a parameter. Note that we expect[10,23] $b \sim 10^{-7}$ cm^3 s^{-1}. The inclusion of excitons in the theory makes no difference to the saturation current if b is very small, regardless of doping, since there is no path for the creation of a significant population of excitons: small values of the binding coefficient prevent the relaxation of many electron-hole pairs to the exciton state. Hence, the theory including excitons agrees with that neglecting them when $b \to 0$ and $G_x = 0$. For larger b we note a reduction in the saturation current, particularly for doping of 10^{18} cm^{-3} for which it is reduced by up to 30%. In order to explain the divergence of J_0/J_0' from unity at high doping values, we note that examination of the ratio of Eqs. (15) and (16) for high b reveals that in this exciton-dominant system
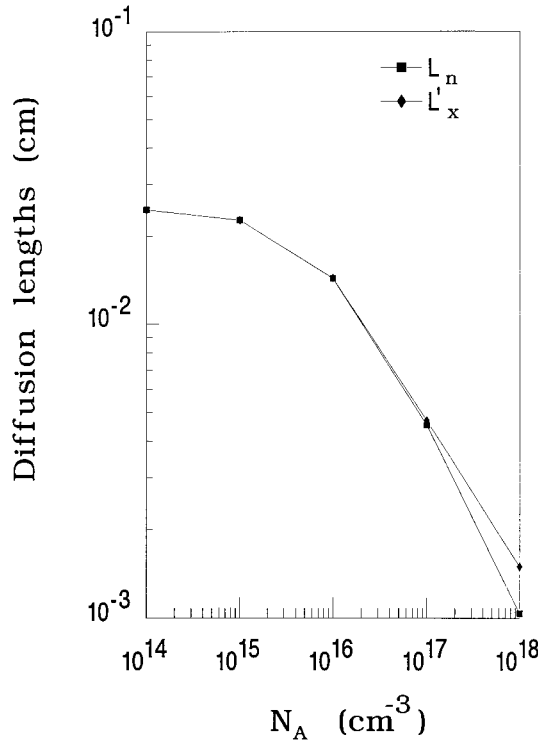
$$J_0/J_0' \approx L_n/L_x'. \qquad (31)$$

FIG. 3. Effective diffusion length for excitons, $L_x' = \epsilon_-^{-1/2}$, and the diffusion length for electrons, L_n, as a function of doping density for fixed value of the binding coefficient, $b = 10^{-6}$.
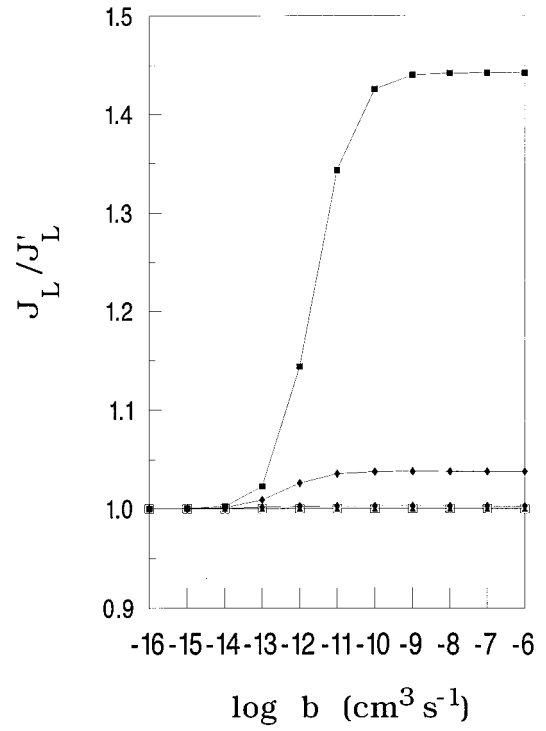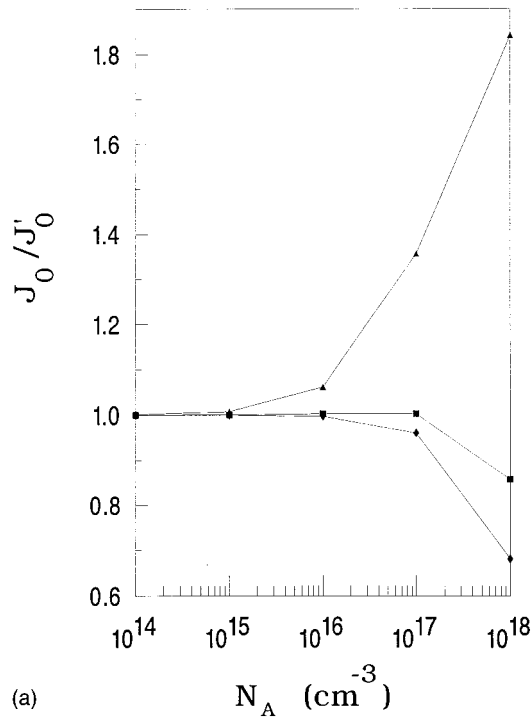

FIG. 4. Ratio of short circuit current with excitons considered to that with excitons neglected as a function of the binding coefficient. The parameter is the doping density, N_A (cm^{-3}): unfilled squares, 10^{15}; triangles, 10^{16}; diamonds, 10^{17}; filled squares, 10^{18}.

As doping is increased, both L_n and L_x' (see Fig. 3) decrease but L_x' falls more slowly than L_n, resulting in a decrease in the current ratio. More generally, the effect of exciton involvement is evident only if the excitonic diffusion length differs from that for minority carriers. The reader may verify using Eq. (11) that $L_x' = \epsilon_-^{-1} = \tau D = L_n$ when we set $\tau = \tau_n = \tau_x$ and $D = D_n = D_x$. In the case illustrated by Fig. 3, the difference between L_n and L_x' when $N_A = 10^{18}$ cm^{-3} can be attributed to $\tau_n \neq \tau_x$ (52%) and $D_n \neq D_x$ (48%).

2. Short circuit current with $G_x = 0, G_{eh} \neq 0$

When $G_x = 0$ excitons are created only through the relaxation of electron-hole pairs. This situation corresponds to spectral regions where exciton absorption is an insignificant fraction of the total absorption.[24] Figure 4 shows the ratio of short circuit current with excitons considered [see Eq. (25)] to that with excitons neglected [see Eq. (26)], assuming $\tau_x(0) = 10^{-4}$ s. For large values of the binding coefficient and for doping of 10^{18} cm^{-3} we calculate that excitons improve the short circuit current by up to 44%.

3. Sensitivity to exciton lifetime

Since our value[10] of $\tau_x(0)$ is uncertain due to the lack of experimental data, we investigate the sensitivity for our results to this parameter. Figures 5(a) and 5(b) show the ratios J_0'/J_0' and J_L/J_L' as functions of doping density for a fixed value of $b = 10^{-7}$ cm^3 s^{-1} for $\tau_x(N_A) = \tau_n(N_A)$ (i.e., $\tau_x(0) = 1.7 \times 10^{-5}$), $\tau_x(N_A) = 10\tau_n(N_A)$, and $\tau_x(N_A) = 0.1\tau_n(N_A)$. When the lifetimes are equal the divergences of the ratios from unity at high doping levels are entirely due to our assumption that $D_x \neq D_n$ since setting $\tau_x = \tau_n$ and

$D_x = D_n$ results in $J_0/J_0' = 1$ and $J_L/J_L' = 1$. The latter result indicates that the fundamental causes of the changes with exciton inclusion are the different lifetimes and diffusivities of excitons and electrons. When $\tau_x > \tau_n$, Fig. 5 shows an improvement in each current ratio and $\tau_x < \tau_n$ causes each to be degraded. This highlights the dependence on exciton diffusion length of the beneficial effects shown in Figs. 2 and 4 and the need for experimental values of exciton parameters.

4. Short circuit current with $G_x \neq 0$

For certain ranges of wavelength near the band edge of an indirect semiconductor the absorption into exciton states is a significant fraction of the total absorption.[24] The short circuit current ratio, J_L/J_L', was recalculated for a fixed doping of $N_A = 10^{18}$ cm^{-3} with G_{x0}/G_{total0} variable between zero and unity and assuming intrinsic lifetime of $\tau_x(0) = 100$ μs. The results are shown in Fig. 6. Of particular note is the very large increase in short circuit current when b is small and a large fraction of the total generation is of excitons rather than carrier pairs. In this situation, the small value of b prevents most of the optically generated excitons from dissociating into carrier pairs and our assumed values for lifetimes and diffusion coefficients yield $L_x/L_n = 3.33$, equal to the factor of improvement in current for small b when $G_{x0}/G_{total0} = 1$. In other words, the cell's collection volume is multiplied by 3.33 under the present assumptions when the diffusion of excitons dominates that of electrons. For larger, and more realistic, values of the binding coefficient many of the optically generated excitons dissociate and the effective collection volume decreases. Hence, if b is actually near its calcu-

(a)
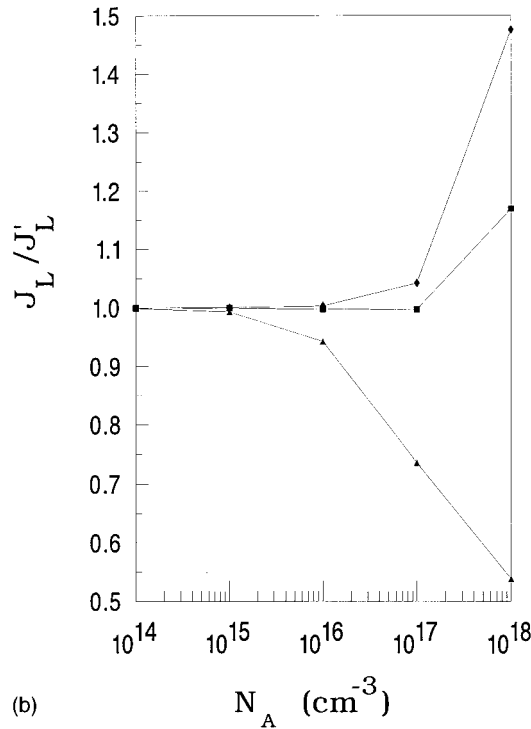
(b)

FIG. 5. Effect of varying exciton lifetime on the ratio of (a) dark saturation current density and (b) short circuit current density with excitons considered to that with excitons neglected as a function of doping density. A fixed value of $b = 10^{-7}$ is assumed. The parameter is the ratio of exciton to carrier lifetime: 0.1, triangles; 1, squares; 10, diamonds.
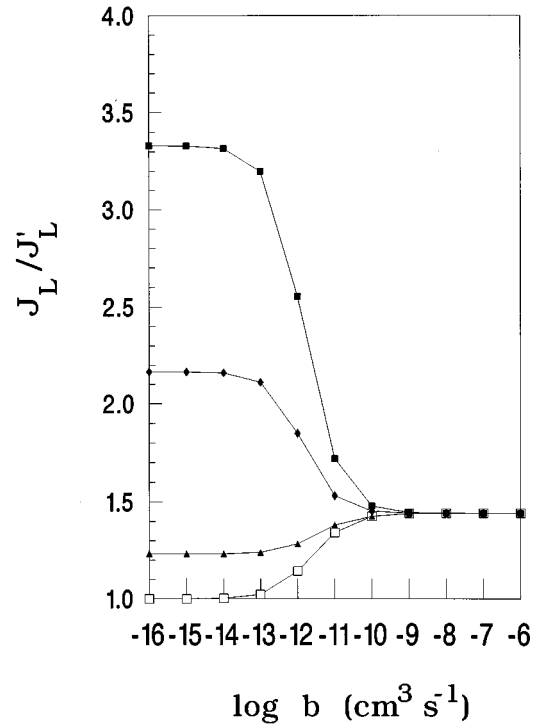

FIG. 6. Ratio of short circuit current density with excitons considered to that with excitons neglected as a function of the binding coefficient for fixed doping density of 10^{18} cm^{-3}. The parameter is the fraction of the optical generation which is of excitons: unfilled squares, 0%; triangles, 10%; diamonds, 50%; filled squares, 100%. The open squares in this graph correspond to the filled squares in Fig. 4.

lated values[10,23] no additional[25] structure due to exciton current contributions would be expected in the spectral response spectrum where G_{x0}/G_{total0} is high.

This suggests a method by which the involvement of exciton transport at room temperature could be confirmed and a range for b might be found experimentally. If b is

actually in the range $b \lesssim 10^{-12}$ cm^3 s^{-1} and if the exciton diffusion length is significantly longer than that of electrons we would expect to see some positive impact of excitonic current contributions on the spectral response of heavily doped solar cells. Effects would be manifested in spectral ranges where excitonic generation is a significant fraction of the total generation. A study of the indirect absorption edge of silicon[24] showed that this condition is met where strong excitonic absorption components are superimposed on an otherwise relatively weak absorption spectrum. In particular, the onset of optical absorption, which is mediated by TO phonon absorption, produces G_{x0}/G_{total0} values up to ~0.5 while the TO plus Raman phonon set's contribution yields G_{x0}/G_{total0} up to ~0.8. Figure 7 gives, for base doping of 10^{18} cm^{-3}, a guide to the current improvements which would be expected in the spectral region dominated by the latter phonon set. Since the threshold for an excitonic absorption component mediated by phonon absorption is given by[24] $E_g(T) - \Delta E_{g,app} - E_x(T,N_A) - E_p$, where E_g is the indirect band gap, $\Delta E_{g,app}$ is the apparent band gap narrowing due to excitons,[4] and E_p is the energy of the phonon set, the enhanced spectral response would be expected to have its threshold at a photon energy of 0.9875 eV, assuming a doping density of 10^{18} cm^{-3}. Additional, weaker enhancements would be expected above the thresholds for optical absorption components mediated by other phonon sets, especially the TO phonon whose threshold is at 1.0657 eV. For clarity, thermal broadening[24] has not been included in the curves presented in Fig. 7 and measured spectra will have a less
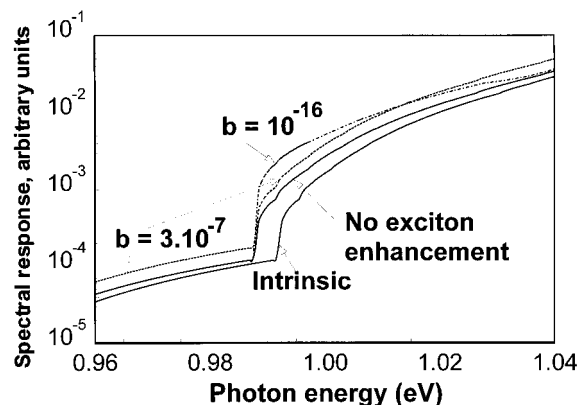
FIG. 7. Theoretical spectral response, without thermal broadening, of silicon which is undoped (lowest curve) and doped to 10^{18} cm^{-3}. The "No exciton enhancement" line is for doped silicon in which excitons are assumed to make no contribution to the current. The curve labeled $b = 3.10^{-7}$ was calculated assuming all parameter values as proposed in Sec. III A 2 and that labeled $b = 10^{-16}$ was calculated using a very low value, $b = 10^{-16}$ cm^3 s^{-1} for the exciton binding parameter. The latter curve follows the No exciton enhancement line at low photon energies.

FIG. 8. G_{x0}/G_{total0} values obtained by dividing the excitonic part (proportional to the square root of photon energy) of the TO plus Raman phonon set absorption spectrum by the total absorption spectrum. Thermal broadening was excluded from the calculation of the spectra.

distinct shape than shown. The lowermost curve was calculated in the same way as the theoretical absorption coefficient[26] in the earlier work,[24] except that the exciton energy has been corrected for room temperature (see Sec. III A 2). It models the spectral response of a lightly doped cell. The solid line models a cell in which the base is doped to 10^{18} cm^{-3}, but there is no enhancement of short circuit current by the transport of excitons. Here, the spectrum has been shifted for the effect of the doping level on exciton energy (see Eq. 28) and for the apparent band gap narrowing (13.8 meV in this case). The curve labeled "$b = 3e\text{-}7$" models the spectral response we would expect if the binding parameter is equal to Nolle's estimate and the other parameters are as assumed in Sec. III A 2 above. In this case, we see from Fig. 6 that the current enhancement is independent of the variation of G_{x0}/G_{total0} with photon energy and the spectral response is simply scaled up by a constant factor of 1.442, the value obtained from Fig. 6. For the curve labeled '$b = 1e\text{-}16$' in Fig. 7, the binding parameter is assumed to be much lower ($b = 10^{-16}$ cm^3 s^{-1}) and other parameters are as for the previous case. For this situation, Fig. 6 indicates that the current enhancement strongly depends on G_{x0}/G_{total0}, so it was necessary to estimate that ratio at each value of photon energy (Fig. 8) and use Eqs. (25) and (26) to calculate the current enhancement, J_L/J_L' at each point.[27] The "$b = 1e\text{-}16$" curve of Fig. 7 is equivalent to that for no enhancement for photon energies below the (TO+Raman) excitonic absorption threshold since $J_L/J_L' = 1$ for this value of b when there is negligible absorption into exciton states (Fig. 6).

Hence, the involvement of exciton transport may be confirmed by the comparison of spectral responses for lightly and heavily doped cells and the value of b may be estimated from the magnitude of the (TO+Raman) "step" in the spectral response so long as the exciton lifetime and diffusivity are known. Since the spectral response improvements are due to an effective increase in the active volume of the solar cell, it is important that the cell(s) used for such an experi-
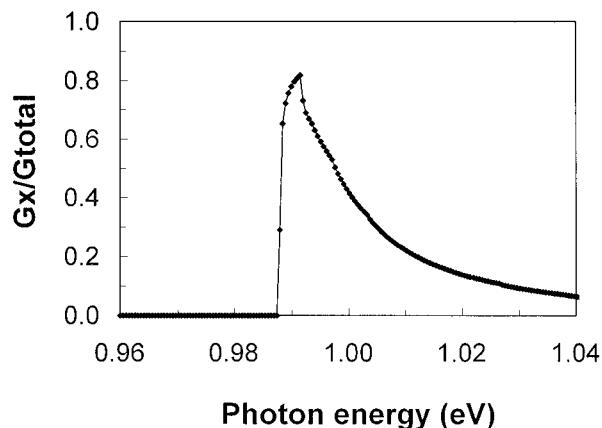
ment have base thickness greatly exceeding the electron diffusion length. Ideally, in order for the current enhancements shown in Fig. 7 for $b = 10^{-16}$ cm^3 s^{-1} to be fully realized, the base thickness must exceed 3.33 times the electron diffusion length if we accept the parameter values cited in Sec. III A 2.

Another technique which may provide evidence for exciton transport at room temperature is the comparison of spectral response on either side of the doping density at which the Mott transition occurs. If the exciton diffusion length is significantly different from the minority carrier diffusion length there should be a sharp change in the spectral response intensity when doping is changed from immediately below the transition density, where exciton contributions are maximized, to just above it, where the excitonic levels have merged into the continuum. In interpreting the results of such an experiment, one would need to consider band gap narrowing due to heavy doping.[28]

IV. CONCLUSIONS

We have developed a theoretical basis for the incorporation of a third type of particle, the free exciton, into a generalized theory of transport in semiconductors and demonstrated this theory by its application to simplified cases of junction diode and solar cell operation. Expressions are given for minority carrier and exciton distributions in the bulk of the base in the dark under the influence of uniform generation and for the dark saturation and (lighted) short circuit currents. Using the best available information on room temperature parameters for excitons, we applied the theory to silicon cells to predict that in the absence of other effects which might counteract the exciton effects, excitons may reduce dark saturation current by up to 30% and simultaneously improve light-generated current by up to 44%. These changes are entirely dependent on the difference in exciton and minority carrier diffusion lengths. Confidence in the numerical results is limited by our reliance on values for room-temperature properties of excitons which have not yet been confirmed by experiment. In particular, we would pre-

fer to have verified values for exciton lifetime, diffusion coefficient, binding coefficient, and equilibrium constant at 300 K. Our model shows that excitons cause an *increase* in saturation current and *decrease* in light-generated current when the exciton diffusion length is assumed shorter than that of the minority carriers. This work includes suggestions for experimental methods to confirm exciton involvement and to estimate the value of the exciton binding parameter from room-temperature spectral response measurements on solar cells.

It should be noted that excitons are, presumably, active in present devices which were designed without their consideration and that excitons already contribute to their characteristics. This work opens up the possibility of optimizing their involvement if the exciton parameters can be reliably quantified.

ACKNOWLEDGMENTS

APPENDIX

In order to solve the coupled differential equations,[13] Eq. (8), we require a nonsingular matrix, P, such that

$$P^{-1}MP = \begin{bmatrix} \epsilon_- & 0 \\ 0 & \epsilon_+ \end{bmatrix} \tag{A1}$$

and

$$\begin{bmatrix} \Delta n \\ \Delta n_x \end{bmatrix} = P \begin{bmatrix} \Delta n' \\ \Delta n_x' \end{bmatrix}, \tag{A2}$$

where $\Delta n'$ and $\Delta n_x'$ are temporary variables. The matrix, P, may be used to diagonalize M, so long as the electron–exciton system is not either decoupled or coincident (i.e., we need $b \neq 0$ and $M_{11} \neq M_{22}$). The columns of P are the eigenvectors corresponding to each of the eigenvalues. Hence, P is given by

$$P = \begin{bmatrix} M_{12} & M_{12} \\ \epsilon_- - M_{11} & \epsilon_+ - M_{11} \end{bmatrix} \tag{A3}$$

and its inverse is

$$P^{-1} = \frac{1}{M_{12}\delta^{1/2}} \begin{bmatrix} \epsilon_+ - M_{11} & -M_{12} \\ M_{11} - \epsilon_- & M_{12} \end{bmatrix}. \tag{A4}$$

These matrices may be used to transform the coupled equations of Eq. (8) into a decoupled pair

$$\frac{d^2}{dx^2} \begin{bmatrix} \Delta n' \\ \Delta n_x' \end{bmatrix} = \begin{bmatrix} \epsilon_- & 0 \\ 0 & \epsilon_+ \end{bmatrix} \begin{bmatrix} \Delta n' \\ \Delta n_x' \end{bmatrix} + P^{-1} \begin{bmatrix} \Gamma_n(z) \\ \Gamma_x(z) \end{bmatrix}. \tag{A5}$$

In the homogeneous case, Eq. (A5) has solutions

$$\begin{bmatrix} \Delta n' \\ \Delta n_x' \end{bmatrix} = \begin{bmatrix} A_{11}\exp(\epsilon_-^{1/2}z) + A_{12}\exp(-\epsilon_-^{1/2}z) \\ A_{21}\exp(\epsilon_+^{1/2}z) + A_{22}\exp(-\epsilon_+^{1/2}z) \end{bmatrix}, \tag{A6}$$

which, when both sides are multiplied on the left by P and after application of the boundary conditions, yields Eqs. (12) and (13) in the text. In the inhomogeneous case,

$$\begin{bmatrix} \Delta n' \\ \Delta n_x' \end{bmatrix} = \begin{bmatrix} \{(\epsilon_+ - M_{11})G_n/D_n - M_{12}G_x/D_x\}\exp(-\alpha z)/\{M_{12}\delta^{1/2}(\epsilon_- - \alpha^2)\} \\ \{(M_{11} - \epsilon_-)G_n/D_n + M_{12}G_x/D_x\}\exp(-\alpha z)/\{M_{12}\delta^{1/2}(\epsilon_+ - \alpha^2)\} \end{bmatrix}, \tag{A7}$$

which transforms to the particular solutions of Eqs. (17) and (18) in the text.

[1] N. Karl, A. Bauer, J. Hopzaepfel, J. Marktanner, M. Moebus, and F. Stoelzle, Mol. Cryst. Liq. Cryst. Sci. Technol. A **252–253**, 243 (1994).

[2] See, for example, J. P. Wolfe, Phys. Today, March, p. 46 (1982).

[3] A. Hangleiter and M. H. Pilkuhn, in *Proceedings of the Seventeenth International Conference on Physics of Semiconductors*, edited by James D. Chadi and Walter A. Harrison, San Francisco, 1984 (Springer, New York, 1985), pp. 1375–1378; A. Hangleiter, *Proceedings of the Thirteenth International Conference on Defects in Semiconductors*, edited by L. C. Kimerling and J. M. Parsey, Jr., Coronado, 1984 (Metallurgical Soc. of AIME, New York, 1985), pp. 213–219, Alternative reference for latter paper: J. Electron. Mater. **14a**, 213–219.

[4] D. E. Kane and R. M. Swanson, J. Appl. Phys. **73**, 1193 (1993).

[5] N. F. Mott, *Metal-Insulator Transitions* (Taylor and Francis, London, 1974), pp 124–169.

[6] Robert S. Knox, *Theory of Excitons*, Solid State Phys., Suppl. 5 (Academic, New York, 1963), pp. 176–181.

[7] Andreas Hangleiter, Phys. Rev. B **35**, 9149 (1987); **37**, 2594 (1988).

[8] M. A. Green, *Silicon Solar Cells. Advanced Principles and Practice* (Bridge, Sydney, 1995), pp. 81–83.

[9] Daniel S.-P. Chan, Bachelor of Engineering thesis, University of New South Wales, School of Electrical Engineering, 1994.

[10] E. L. Nolle, Sov. Phys. Solid State **9**, 90 (1967).

[11] The parameters, b and n^*, correspond to γ_e and α/γ_e, respectively, in the formulation of Ref. 10 and to W_{d1} and W_{1d}/W_{d1} in Ref. 23 and n^* corresponds to N_e in M. Combescot, Phys. Status Solidi B **86**, 349 (1978).

[12] Martin A. Green, *Solar Cells Operating Principles and System Applications* (Prentice-Hall, Englewood Cliffs, NJ, 1982), reprinted by the University of NSW in 1986 and 1992, Chap. 4, pp. 62–84.

[13] See, for example, Gilberg Strang, *Linear Algebra and its Applications* (Academic, New York, 1976), Chap. 5; or Henry G. Jacob and Duane W. Bailey, *Linear Algebra* (Houghton Mifflin, Boston, 1971), pp. 304–308.

[14] A. B. Sproul and M. A. Green, J. Appl. Phys. **70**, 846 (1991).

[15] Jerry G. Fossum, Solid-State Electron. **19**, 269 (1976).

[16] A. W. Stephens and M. A. Green, J. Appl. Phys. **74**, 6212 (1993).

[17] K. L. Shaklee and R. E. Nahory, Phys. Rev. Lett. **24**, 942 (1970).

[18] A. Hangleiter and R. Häcker, Phys. Rev. Lett. **65**, 215 (1990). Unpublished work in progress at UNSW suggests that $E_{x\infty}$ may actually be close to 15 meV at 300 K due to corrected dependencies of effective masses with temperature.

[19] N. F. Mott, *Metal Insulator Transitions* (Barnes & Noble, New York, 1974).

[20] George B. Norris and K. K. Bajaj, Phys. Rev. B **26**, 6706 (1982).

[21] M. A. Tamor and P. Wolfe, Phys. Rev. Lett. **44**, 1703 (1980); B. Laurich, H. Hillmer, and A. Forchel, J. Appl. Phys. **61**, 1480 (1987).

[22] H. Gummel and M. Lax, Ann. Phys. **2**, 28 (1957); M. Lax, Phys. Rev. **119**, 1502 (1960).

[23] J. Barrau, M. Heckmann, J. Collet, and M. Brousseau, J. Phys. Chem. Solids **34**, 1567 (1973).

[24] Richard Corkish and Martin A. Green, J. Appl. Phys. **73**, 3988 (1993).

[25] The spectral regions where G_x/G_{total} is high are among those where the thresholds of excitonic absorption create "humps" in the absorption spectrum (see Ref. 24). If b is in the expected range we expect no structure in addition to that discussed in the earlier work.

[26] M. J. Keevers and M. A. Green, Appl. Phys. Lett. **66**, 174 (1995) show that band-to-band absorption coefficient and internal quantum efficiency (IQE) are proportional for weak absorption and that spectral response is proportional to IQE if only a narrow spectral range is considered and the surface reflectance varies negligibly over that range.

[27] In order to obtain an initial estimate of the impact of excitons, $\alpha=0$ was used in these equations since $\alpha<0.1$ cm^{-1} for the energy range considered. A more complete treatment would use the appropriate value of α at each photon energy.

[28] Karl W. Böer, *Survey of Semiconductor Physics* (Van Nostrand Reinhold, New York, 1990), pp. 236–240.